



Saturated permeability behavior of biochar-amended clay

Wen-Jing Sun^{1,2} · Ming-Yu Li¹ · Wen-Jie Zhang¹ · Yun-Zhi Tan^{2,3}

Received: 7 February 2020 / Accepted: 9 July 2020 / Published online: 16 July 2020
© Springer-Verlag GmbH Germany, part of Springer Nature 2020

Abstract

Purpose Biochar has the characteristics of loose porosity, high specific surface area, and strong adsorption properties. Recently, the compacted biochar amended clay has been proposed as a sustainable alternative material for the final cover of landfills. However, the effect of biochar on saturated hydraulic conductivity (k_{sat}) is not yet conclusive. The objective of this study was to determine the influence of biochar content on the permeability of biochar-clay mixed soils.

Materials and methods The clay used in the study belongs to the low liquid limit clay. The biochar is produced by heating the rice straw under an oxygen-deficient condition at a temperature of 500 °C. To study the effect of biochar content on the permeability of biochar-clay mixed soils, the biochar-clay mixed soils with the mass percentage of biochar being 0%, 5%, 10%, 15%, and 20% were used. The saturated hydraulic conductivity of the biochar-clay mixed soils was measured by the head pressure control permeameter. Meanwhile, the micro-pore structure of the saturated biochar-clay mixed soils was obtained by the nuclear magnetic resonance (NMR) technique.

Results and discussion It can be observed that the saturated hydraulic conductivity k_{sat} of biochar-clay mixed soils increases linearly as the biochar content increases. The NMR results show that the T_2 distribution curve of pure clay is a unimodal pattern, while the T_2 distribution curve of biochar-clay mixed soils presents the bimodal pattern, where T_2 is the transverse relaxation time, reflecting the pore size of the soil specimens. With the increase of biochar content, the T_2 spectrum of the mixed soils moves slightly to the right, and T_2 at main peak increases gradually, correspondingly the most probable pore size of biochar-clay mixed soils increases.

Conclusions The pore size distribution of the soil was changed by the addition of biochar and subsequently affects the permeability of biochar-clay mixed soils. This study provides some useful suggestions for optimizing the pore structure of the biochar amended clay anti-seepage layer in the final cover of landfills.

Keywords Biochar-clay mixed soils · Saturated hydraulic conductivity · Nuclear magnetic resonance · Micro-pore structure · Most probable pore size

Responsible editor: Hailong Wang

✉ Wen-Jie Zhang
wjzhang2006@shu.edu.cn

¹ Department of Civil Engineering, School of Mechanics and Engineering Science, Shanghai University, Shanghai 200444, People's Republic of China

² Hubei Key Laboratory of Disaster Prevention and Mitigation (China Three Gorges University), Yichang 443002, People's Republic of China

³ College of Civil Engineering & Architecture, China Three Gorges University, Yichang 443002, People's Republic of China

1 Introduction

The landfill final cover is conducive to controlling and reducing the infiltration of rainwater. Many countries have put strict restrictions on the saturated hydraulic conductivity (k_{sat}) of the landfill final cover, and the minimum k_{sat} of the cover layer varies in different countries. For example, k_{sat} should be less than 1.0×10^{-7} cm/s in the USA (Bareither et al. 2020), in China (GB 51220–2017), and 1.0×10^{-6} cm/s in Korean (Kwon and Cho 2011). Because of low permeability, the compacted clay anti-seepage layer has been widely used as a barrier layer for the final cover of landfills (US EPA 1989). However, the shrinkage and cracking of traditional compacted clay cover decrease the permeability of the anti-seepage barrier, owing to the climate change and ground settlement (Horn

et al. 2014). Therefore, a sustainable and environmentally friendly soil-amended material, namely biochar, has received wide attention from many researchers. As a carbon-rich substance produced by heating biomass, the biochar is characterized by lower density, the higher specific surface area, higher ion exchange capacity, and stability (Jeffery et al. 2011; Zornoza et al. 2016). The addition of biochar to soil can reduce the density, increase the porosity, and subsequently alter the permeability and the water retention capacity of soil (Laird et al. 2010; Lu et al. 2014; Zhao et al. 2015a; Villagra-Mendoza and Horn 2018; He et al. 2019; Peng et al. 2019).

At present, the permeability of biochar amended soils has been studied by many researchers; however, the effect of biochar on saturated hydraulic conductivity (k_{sat}) of clay with high degree of compaction is not yet understood. Laird et al. (2010) found that the addition of biochar had no obvious effect on the hydraulic property of soil. Oguntunde et al. (2010) found that the saturated hydraulic conductivity of the biochar mixed soil increased remarkably by 88% compared with that of the soil without biochar. Lei and Zhang (2013) studied the effect of biochar derived from different pyrolysis temperatures on soil saturated hydraulic conductivity, with results indicating that biochar applications improved the conductivity. Notably, the influence of increased biochar produced by high-temperature pyrolysis on soil saturated hydraulic conductivity was more apparent. Ajayi et al. (2016) studied the effects of biochar on the permeability of two different types of soils (fine sand and sandy loamy silt). The results indicated that the saturated hydraulic conductivity of the sandy loamy silt increased with the increase of biochar content. However, the saturated hydraulic conductivity of the fine sand decreased with the increase of biochar content. Villagra-Mendoza and Horn (2018) studied the effects of biochar on the permeability of sand and sandy loam. The results indicated that the saturated hydraulic conductivity of sand and sandy soil decreased after adding biochar, and the decrease of k_{sat} was more pronounced in the sandy mixtures than in the sandy loam. Devereux et al. (2012) found that the saturated hydraulic conductivity decreased with the increase of biochar content. After adding 5% biochar to the soil, it was found that the saturated hydraulic conductivity decreased from 4.8×10^{-3} to 2.3×10^{-3} cm/s. The effect of biochar application on hydraulic properties of soil was also investigated by Ibrahim et al. (2013). In their tests, the saturated hydraulic conductivity was found to decrease under the application of biochar. Barnes et al. (2014) studied the permeability of three different soils modified by biochar (i.e., sand, organic-rich topsoil, and clay-rich soil) and found that biochar amendment decreased saturated hydraulic

conductivity by 92% in sand and 67% in organic soil, but increased by 328% in clay-rich soil.

To sum up, different variation tendencies of permeability can be observed from above test results after adding biochar into soil, and the reason for the difference is assumed to be related to the physical and chemical properties of the soil itself, and the pore structure of biochar prepared by disparate biomass feedstock and pyrolysis temperature, and also the mutual adaptive evolutions of micro-pore structure between soil and biochar. Therefore, it is of necessity to study the influence of pore structure on the permeability of biochar-amended soils.

The objective of this paper is to explore the effect of biochar content on the permeability of biochar-clay mixed soils. For this, the saturated hydraulic conductivity (k_{sat}) of biochar-clay mixed soils with different biochar content (i.e., 0%, 5%, 10%, 15%, and 20%) was measured by adopting a head pressure control permeameter. Next, the micro-pore structures of biochar-clay mixed soils with different biochar content were also obtained by using NMR technique without destroying the pore structure. Then, the effect mechanism of biochar content on the permeability of biochar-clay mixed soils was analyzed. Finally, the differences and their causes of the saturated hydraulic conductivity of different types of soils mixed with biochar were discussed by analyzing the test results.

2 Materials and methods

2.1 Test materials

The clay used in the test belongs to the low liquid limit clay in line with the classification plastic diagram of fine-grained soil. The biochar used in the test is produced by heating the rice straw under an oxygen-deficient condition at a temperature of 500 °C. The basic physical properties of clay and biochar used in the test are listed in Tables 1 and 2. The ash content in the biochar is 18.8% by means of ASTM D1762–84 (2007). Twenty grams of biochar is placed in the muffle furnace at a temperature of 800 °C for 4 h and the quality loss is obtained.

After the biochar particles are sieved through a 200-mesh sieve, the biochar with a particle size of less than 74 μm is prepared for use. The particle gradation curve of screened biochar is illustrated in Fig. 1. The grain size distribution curve of clay is also presented in Fig. 1. The particle size larger than 74 μm is measured by using the sieving method in ASTM

Table 1 Basic properties of tested clay

Clay	Specific gravity G_s	Liquid limit w_L (%)	Plastic limit w_P (%)	Plasticity index I_p
	2.67	35.98	22.20	13.78

Table 2 Basic properties of tested biochar

Biochar type	Specific gravity G_s	Specific surface area SSA (m^2/g)	Bulk density ρ (g/cm^3)	Ash content (%)
Rice straw	1.99	385.60	0.55	18.80

D422–63 (1998), and the rest part is measured by the use of the laser particle size analyzer.

The skeleton structure of the original biomass will not be damaged during the high-temperature pyrolysis process, and the microstructure of biochar can be well preserved. Figure 2 depicts the morphological characteristics of the tested biochar by using the SEM tests, in which the porosity of the biochar internal structure can be observed clearly.

2.2 Specimen preparation

To study the effect of biochar content on the permeability of biochar-clay mixed soils, the mixed soils with the mass percentage of biochar being 0%, 5%, 10%, 15%, and 20% were used. To eliminate the influence of ion exchange on the permeability of the soil specimens, the deionized water is used in the test. The specimens with a height of 2.00 cm and a diameter of 3.80 cm were prepared, with initial water content of 14% and dry density of $1.50 g/cm^3$.

The water content of 14% was selected, mainly considering the natural water content of the landfills final cover. It should be noted that the water content is re-measured before specimen preparation. In order to get the same dry density, the particle density of biochar and clay was determined in advance, and the particle density of the mixed soil with different biochar content was obtained. The mass of biochar, clay, and deionized water can be calculated according to the target dry density, water content, and size of the specimen. The preweighted deionized water, oven-dried clay, and biochar are mixed thoroughly in a large pan. After stirred thoroughly,

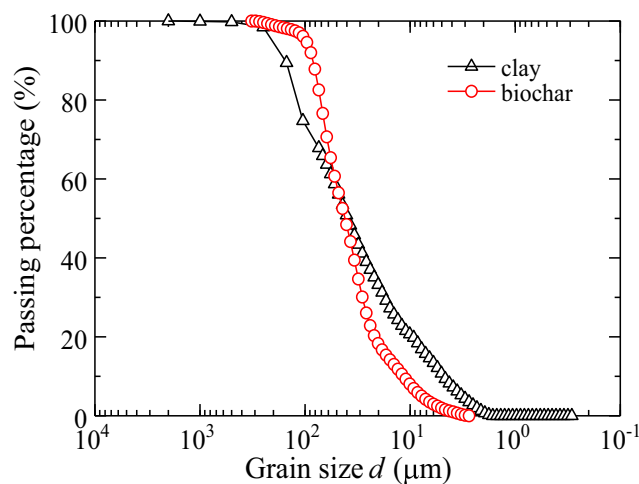


Fig. 1 Grain size distributions of the tested clay and biochar

the mixture was sealed in polyethylene bags for 24 h to reach water homogeneous. Then the compressed specimens with the same dry density were prepared.

2.3 Measurement of saturated hydraulic conductivity

The head pressure control permeameter shown in Fig. 3 was adopted to measure the saturated hydraulic conductivity of the biochar-clay mixed soils. The air pressure was applied to the surface of solution in the gas-liquid separator to form a stable head pressure. An oil layer was set between the gas and the liquid to prevent the gas from dissolving in solution. During the test, the test head pressure was set to 50 kPa (equivalent to 5 m water head between the two end of specimen). The water outlet of the gas-liquid separator was connected with the water inlet at the bottom of the permeameter. Deionized water can be uniformly infiltrated into the soil specimen through the porous disc as air pressure was applied. When the solution seeped out from the soil specimen, the outflow solution was collected in a needle tubing and mass weighed at regular intervals.

The saturated hydraulic conductivity of soil specimen can be determined by the following equation:

$$k_{sat} = \frac{\Delta Q \cdot L}{A \cdot \Delta h \cdot \Delta t} \tag{1}$$

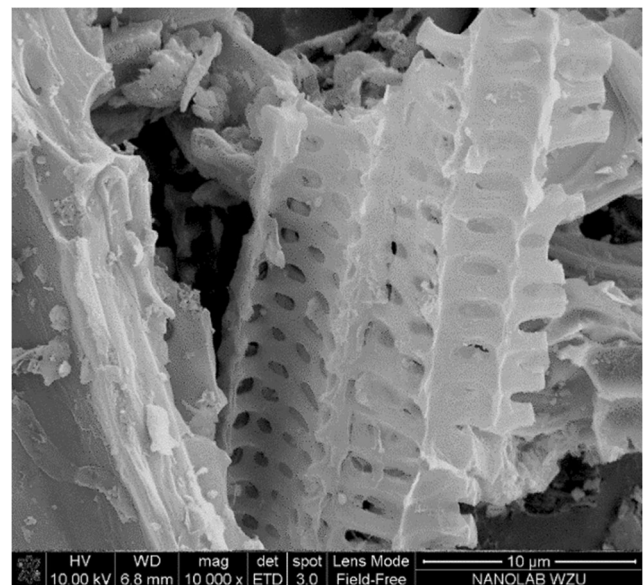
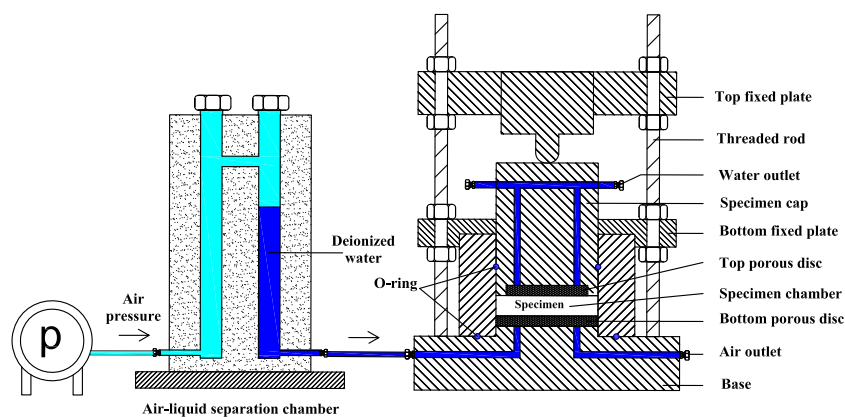


Fig. 2 Morphological characteristics of tested biochar. **a** Picture of test apparatus. **b** Schematic diagram of test apparatus

Fig. 3 Picture and schematic diagram of the head pressure control permeameter



(a) Picture of test apparatus



(b) Schematic diagram of test apparatus

where k_{sat} is the saturated hydraulic conductivity (cm/s); L is the height of the specimen (cm); A is the cross-sectional area of specimen (cm²); Δt is the interval of time (s); ΔQ is the quantity of flow for a given time interval (cm³); Δh is the height of water head (cm).

2.4 Micro-pore structure investigation by NMR technique

At present, the following three test methods are commonly adopted to investigate the micro-pore structure of soils, i.e., the mercury intrusion porosimetry (MIP) test, the nitrogen adsorption volume (NAV) method, and the nuclear magnetic resonance (NMR) technique (Xi et al. 2016; Chen et al. 2019; Zhao et al. 2015b). In MIP and NMR tests, the sample needs to be freeze-dried and sublimated before the micro test. During the freeze-drying process, the pore water of soil sample is frozen, and subsequently expands in volume; the pore structure of soil sample was destroyed. Moreover, when the MIP or NMR test is performed, the saturated biochar-clay mixed soils are easily crushed for its lower bonding strength

of granules, especially in the high pressure stage. Therefore, the MIP and NAV tests are not suggested to test the micro-pore structure of biochar-clay mixed soils in this study. However, the NMR technique is proved to be an effective testing method to measure the micro-pore structure of soils, with some advantages of rapid, accurate, nondestructive, and good repeatability (Fang et al. 2018).

The MacroMR12-110H-1 Mini NMR analyzer is used to analyze the microstructure of the biochar-clay mixed soils. The device primarily consists of four parts: a permanent magnet, a soil sample tube, a radio frequency system, and a data acquisition-analysis system. The magnetic field strength of the permanent magnet unit is 0.3 T (Tesla). The temperature of the magnet unit is maintained at 32 °C, with a variation of ± 0.01 °C to ensure uniformity and stability of the main magnetic field in the test. Moreover, the effective test area of the sample tube is 60 by 60 mm ($h \times d$, where h and d are the height and diameter of the sample tube, respectively). The echo time is 0.2 ms, the repetition time is 1000 ms, and the number of echoes is 2000.

For a fluid saturated porous, the T_2 relaxation rate $1/T_2$ is proportional to the surface-to-volume (s/v) ratio of the pore

(Coates et al. 1999; Jaeger et al. 2009). Therefore, $1/T_2$ can be simplified as follows:

$$\frac{1}{T_2} = \rho_2 \left(\frac{s}{v} \right)_{\text{pore}} \tag{2}$$

where ρ_2 is the lateral transverse relaxation rate that is bound up with the physical and chemical properties of soils (Coates et al. 1999); s and v are the surface area and the volume of the pore, respectively. By assuming that the shape of the pores in the soil specimen is ideal and to be cylindrical with the pore radius of r (Tian et al. 2013; Kong et al. 2020), it is believed that Eq. (2) can be simplified approximately as follows:

$$\frac{1}{T_2} \approx \rho_2 \cdot \left(\frac{2}{r} \right)_{\text{pore}} \tag{3}$$

It can be observed from Eq. (3) that the value of the lateral transverse relaxation time T_2 is directly proportional to pore radius r . Therefore, the value of T_2 can be employed to reflect the pore size of soils.

3 Results and analysis

3.1 Relationship between water outflow and outflow time for biochar-clay mixed soils with different biochar content

Figure 4 shows the relationship between the water outflow and outflow time for biochar-clay mixed soils with different biochar content. When the outflow reaches a stable stage, the water outflow increases linearly with the outflow time. As shown in Eq. (1), the ratio $\Delta Q/\Delta t$ is related closely to the saturated hydraulic conductivity. Figure 4 shows that the slope of the outflow vs. time relationship in the stable stage

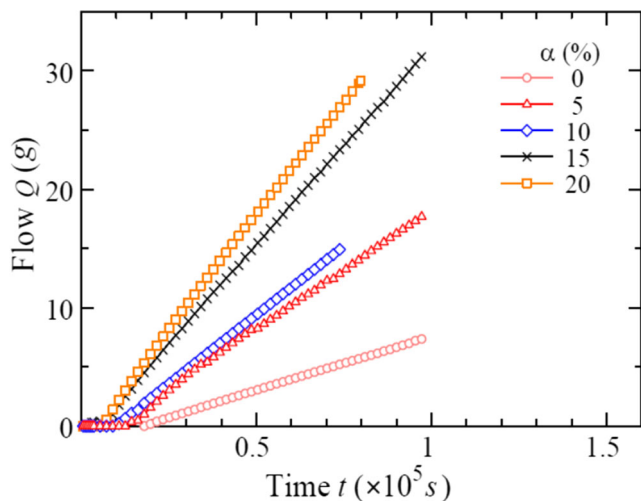


Fig. 4 Relationship of outflow and outflow time of biochar-clay mixed soils with different biochar content

increases with the increase of biochar content. For example, the slope of pure clay is 0.000084, and to mixtures with 5%, 10%, 15%, and 20% biochar content, the slope increases to 0.00019, 0.000233, 0.000332, and 0.000384, respectively. It can be seen that when the biochar content is 20%, the slope in the stable stage is nearly 4.5 times of pure clay, meaning that the permeability of the biochar-clay mixed soils can be significantly enhanced when the biochar is added to soils. In addition, it can also be found in Fig. 4 that the initial outflow time (i.e., the inflection point position of the curve in the diagram) of the biochar-clay mixed soils becomes shorter along with the increase of the biochar content. This also means the increase of porosity of soils with the increase of biochar content.

3.2 Effect of biochar content on saturated hydraulic conductivity of biochar-clay mixed soils

Figure 5 shows the variation of the saturated hydraulic conductivity with biochar content of compacted biochar-clay mixed soils. It can be observed that k_{sat} of biochar-clay mixed soils increases almost linearly as the biochar content increases. For pure clay, the value of k_{sat} is 2.96×10^{-8} cm/s. However, the value of k_{sat} rises to 6.7×10^{-8} , 8.22×10^{-8} , 1.17×10^{-7} , and 1.35×10^{-7} cm/s when the biochar contents are 5%, 10%, 15%, and 20%, respectively. Compared with the pure clay specimen, the value of k_{sat} increases by about 4.5 times for the biochar-clay mixed soil with 20% biochar content. However, it still meets the requirements of the saturated hydraulic conductivity in the technical specification for landfill final cover of municipal solid waste (GB 51220–2017).

The test results of this paper are compared with the previous studies on the permeability of biochar-amended soils, as shown in Table 3. Yaghoubi (2011) studied the saturated hydraulic conductivity of biochar-amended clay with the dry density of 1.60 g/cm^3 . It was found that the saturated hydraulic conductivity increased first and then decreased with the

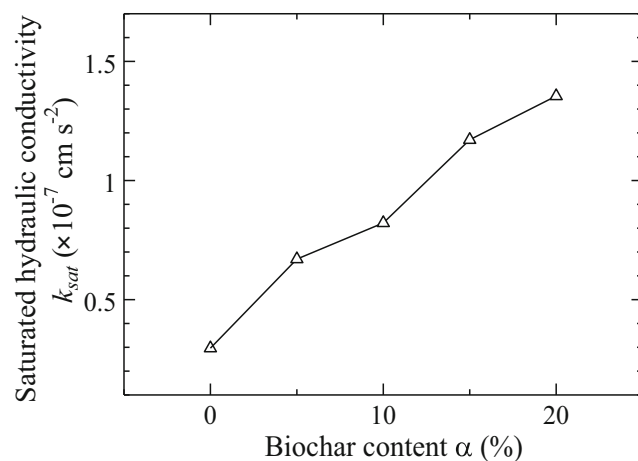


Fig. 5 Variation of the saturated hydraulic conductivity of compacted biochar-clay mixed soils with biochar content

Table 3 Effect of biochar on the saturated hydraulic conductivity of biochar-amended soils

	ρ_d (g/cm ³)	Type	α (%)					Reference
			0	5	10	15	20	
k_{sat} (cm/s)	1.50	Biochar + clay	2.96×10^{-8}	6.70×10^{-8}	8.20×10^{-8}	1.17×10^{-7}	1.35×10^{-7}	This paper
	1.60	Biochar + clay	4.30×10^{-9}	5.70×10^{-8}	6.50×10^{-7}	–	1.80×10^{-7}	Yaghoubi 2011
	1.14	Biochar + clay	1.20×10^{-7}	2.10×10^{-7}	–	–	1.30×10^{-6}	Wong et al. 2018
	1.38	Biochar + sand	2.90×10^{-4}	–	2.30×10^{-5}	–	–	Barnes et al. 2014
	1.39	Biochar + clay	3.20×10^{-6}	–	1.20×10^{-5}	–	–	Barnes et al. 2014

increase of biochar content. When the biochar content is 20%, the saturated hydraulic conductivity decreases. Wong et al. (2018) tested the saturated hydraulic conductivity of biochar-amended kaolin clay with the dry density of 1.14 g/cm³. It was concluded that the saturated hydraulic conductivity increased continuously with the increase of biochar content. Barnes et al. (2014) tested the saturated hydraulic conductivity of biochar-amended sand and biochar-amended clay with dry density of 1.38 g/cm³ and 1.39 g/cm³, respectively. It was found that the saturated hydraulic conductivity decreased for the biochar-amended sand. However, when biochar was added to the clay soil, the saturated hydraulic conductivity increased. It can be observed that there are wide differences in the saturated hydraulic conductivity of different kinds of biochar-amended soils.

4 Results of NMR tests

Figure 6 shows the T_2 distribution curve of biochar-clay mixed soils with different biochar content (0%, 5%, 10%, 15%, and 20%). It can be observed that the T_2 distribution curve of pure clay ($\alpha = 0\%$) is a unimodal structure with the largest peak. Besides, the T_2 value corresponding to the peak of T_2 spectrum is between 1 and 2 ms. The T_2 spectrum of biochar-clay mixed soils with different biochar content shows the bimodal pattern. The first peak (the main peak) appears in the range of 1–2 ms, and the secondary peak (the small peak) appears in the range of 10–100 ms. With the increase of biochar content, the T_2 spectrum of the biochar-clay mixed soils moves slightly to the right. It can be seen that the T_2 distribution range corresponding to the main peak of the specimen added with 0%, 5%, 10%, 15%, and 20% biochar is 0.11 to 5.17 ms, 0.13 to 7.80 ms, 0.14 to 11.89 ms, 0.16 to 14.65 ms, and 0.11 to 16.83 ms, respectively. In addition, T_2 at peak increases with increasing the biochar content, and when the biochar contents are 0%, 5%, 10%, 15%, and 20%, the corresponding T_2 at peak is 1.48 ms, 1.70 ms, 1.83 ms, 2.09 ms, and 2.41 ms, respectively.

The T_2 distribution reflects the pore-size distribution. Yu et al. (2019) showed that the movement of the T_2 spectrum can

reflect the variation tendency of pore size. As it is known from Eq. (3), T_2 is proportional to r ; therefore, the increase of T_2 represents the increase of pore size, and T_2 at main peak of T_2 spectrum symbolizes the most probable pore size (Zhang et al. 2014), that is, the pore radius of those pores with maximum probability.

According to the proportional relationship between T_2 and r , as shown in Eq. (3), and the variation of T_2 spectrum of the biochar-clay mixed soils with different biochar content, as shown in Fig. 6, it can be observed that the T_2 at main peak of T_2 spectrum of biochar-clay mixed soils increases, corresponding the increase of the most probable pore size of soils with the increase of biochar content. It is common practice to categorize the T_2 components below about 3 ms as being associated with clay bound water (Dunn et al. 2002). Prammer et al. (1996) suggested the possibility that the convenient T_2 cutoff at about 3 ms can be used for clay typing. Therefore, T_2 cutoff at about 3 ms was adopted as the boundary between the micropores and meso/macropores. It is known that the area of T_2 distribution curve and horizontal axis can reflect the pore amount. Figure 7 represents the amount of meso/macropores for the biochar-clay mixed soils with different biochar content according to the T_2 distribution curves. It can be observed that the meso/macropores amount

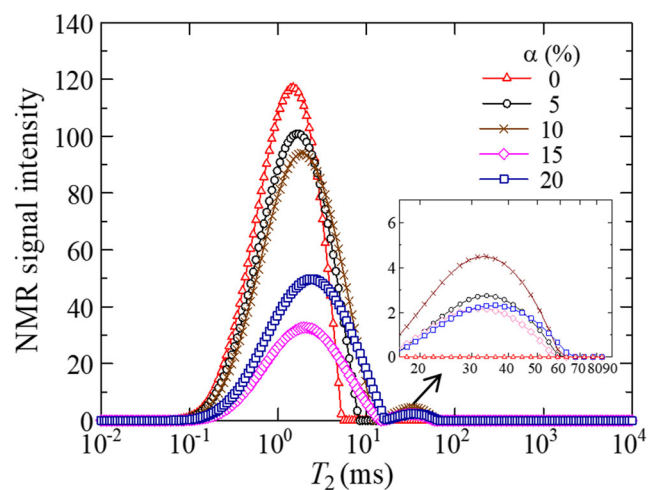


Fig. 6 T_2 distribution curves of biochar-clay mixed soils with different biochar content

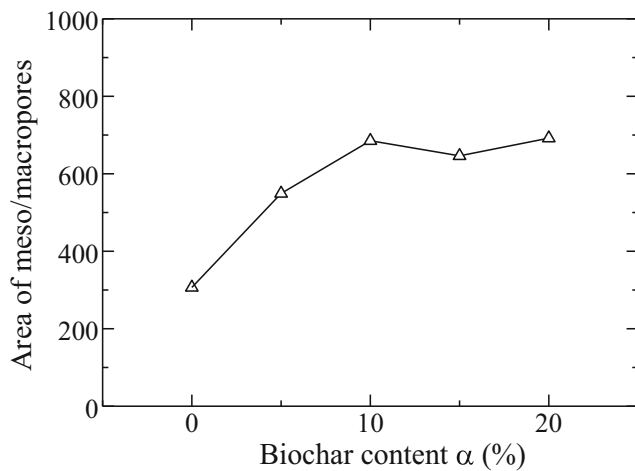


Fig. 7 Meso/macropores amount of biochar-clay mixed soils with different biochar content

increases with biochar content increasing. Generally speaking, the saturated hydraulic conductivity is significantly affected by macropores in soils (Jirku et al. 2013; Ajayi et al. 2016; Fei et al. 2019). Therefore, from the variation of the most probable pore size, as shown in Fig. 7, and the amount of meso/macropores, as shown in Fig. 6, with the biochar content, it can explain the increasing trend of saturated hydraulic conductivity with the increase of biochar content.

5 Discussion

He et al. (2019) studied the effect of biochar on the physical and chemical properties of soils, and concluded that the addition of biochar will not only vary the porosity of soil, but also lead to the reorganization of the aggregation process of soil, which alters the pore size distribution of soil.

In general, the permeability is related to the microstructure of soils, that is, micro-pore structure, particle size distribution of soil, the particle size of biochar, and the relative particle size of biochar and clay. Among them, the influence of the relative particle size of biochar and clay on the micro-pore structure of soils, and subsequently the saturated hydraulic conductivity, is more significant. For clay whose particle size is smaller than or equal to that of biochar, biochar may exist as a part of the soil skeleton of the mixed soils, which increases the porosity of soil and subsequently the saturated hydraulic conductivity. However, for materials whose particle size is larger than that of biochar, such as sand or organic soil, biochar is filled in the particle pores as filler. Hence, the porosity of soil decreases and subsequently the saturated hydraulic conductivity of the mixed soils decreases.

In this study, the effect of biochar content on the saturated hydraulic conductivity of biochar-clay mixed soils was studied. The macroscopic permeability test results showed that the saturated hydraulic conductivity k_{sat} of the biochar-clay mixed

soils increased linearly by adding biochar. That is, the addition of biochar has the potential to improve the permeability of the clay.

The reason may be related to the particle size of biochar and the pore size of clay. It can be obtained from Fig. 1 that the optimal particle size of biochar is about 70 μm , and clay is about 150 μm . Moreover, from MIP results of clay, it can be seen that the optimal pore size distribution of clay is between 0.01 and 1 μm (Chen et al. 2017; Wong et al. 2018). According to these results, the optimal particle size of biochar is generally the same order of magnitude as that of clay; therefore, it can be judged that the distribution mode of biochar is to act as the soil skeleton in the mixtures. Because biochar is porosity and acts as the skeleton of mixture, the porosity of biochar-clay mixed soils increases, which leads to the increase of the saturated hydraulic conductivity. In the results of this paper and Wong et al. (2018), the mixture's saturated hydraulic conductivity increases with the increase of biochar content. For example, Wong et al. (2018) tested the saturated hydraulic conductivity of clay with a compaction degree of 90%, and the results showed that the addition of biochar increases the saturated hydraulic conductivity of compacted kaolin clay.

For soils with particle size is larger than that of biochar, how will the saturated hydraulic conductivity change after adding biochar? Kong et al. (2020) showed that the most probable pore diameter of the standard sand is about 100 μm , which is larger than biochar particle size. Therefore, the pores among sand particles could be filled by biochar, and the water-conducting pores may be clogged, which could cause the decrease of k_{sat} . Villagra-Mendoza and Horn (2018) showed that the saturated hydraulic conductivity of biochar-amended sand and sandy loam decreased, and the saturated hydraulic conductivity of biochar-amended sand decreased more significantly. This is because the particles of sand are larger than those of sandy loam. Barnes et al. (2014) measured the saturated hydraulic conductivity of three kinds of biochar-amended soils. For the coarse soil (sand and organic soil) amended by biochar, the saturated hydraulic conductivity decreased. However, when biochar is added to the clay-rich soil, the saturated hydraulic conductivity increased again. The above study fully showed that the saturated hydraulic conductivity of biochar-amended soils is closely related to the particle size of biochar and the relative particle size of biochar and soil.

Due to different degrees of compaction, the saturated hydraulic conductivity of soils can go in two different directions, although the biochar is added to the same type of soil. For example, Zhao et al. (2015a) tested the saturated hydraulic conductivity of silty clay loam improved by biochar, and found that the addition of biochar reduced the saturated hydraulic conductivity of silty clay loam. However, the research results of this paper and the test results of Wong et al. (2018) showed that the saturated hydraulic conductivity

of biochar-amended clay increases gradually with the increase of biochar content. Zhao et al. (2015a) studied the agricultural silty clay loam; the degree of compaction of soil is generally required to be lower (Garg and Ng 2015). However, in this research and Wong et al. (2018), it is aimed at the final cover of landfills, which requires a high degree of compaction, not less than 90% of maximum dry density (GB 51220–2017). Therefore, the saturated hydraulic conductivity of the same type of soil amended by biochar has the opposite permeability test results.

To sum up, the saturated hydraulic conductivity of biochar amended soils is related to the micro-pore structure of soils, which is connected to the compactness, the particle size of soils and biochar, and pore size distribution of soils.

6 Conclusions

In order to study the effect of biochar content on the permeability of biochar-amended clay soil, the saturated hydraulic conductivity of biochar-clay mixed soils with different biochar content was determined adopting the head pressure control permeameter. Subsequently, the micro-pore structure of the saturated biochar-clay mixed soils was measured using NMR technique. The results show that the addition of biochar changes the micro-pore structure of soil and subsequently affects the permeability of biochar-clay mixed soils.

The saturated hydraulic conductivity of biochar-clay mixed soils has a nearly linear increase with the increase of biochar content. The shape of the T_2 spectrum changes from a unimodal pattern of pure clay to the bimodal one of biochar-clay mixed soils. In addition, the T_2 distribution curve of biochar-clay mixed soils gradually shifted to the right, and the most probable pore size of the mixed soils increased with the increase of biochar content, verifying the macroscopic permeability of biochar-clay mixed soils.

The permeability of soil is related to the microstructure, furthermore, the pore structure, particle size distribution of soil and biochar, and the interaction effect between biochar and clay such as the pore size distribution of mixed soils. The permeability of different types of soils mixed with biochar is quite different.

Acknowledgements The authors are grateful to the National Sciences Foundation of China (Grant No. 41977214, 41572284, 51979150, 41772300) and the Open Research Fund of Hubei Key Laboratory of Disaster Prevention and Mitigation (China Three Gorges University) (Grant No. 2017KJZ01) for the financial supports.

Funding information This study is financially supported by the National Sciences Foundation of China (Grant Nos. 41572284, 41977214, 51979150, 41772300) and the Open Research Fund of Hubei Key Laboratory of Disaster Prevention and Mitigation (China Three Gorges University) (Grant No. 2017KJZ01).

Compliance with ethical standards

The authors wish to confirm that the contents of this manuscript have not been published previously and the manuscript is not under consideration for publication elsewhere.

Conflict of interest The authors declare that they have no conflict of interest.

Research involving human participants and/or animals The authors wish to confirm that there is no research involving human participants and/or animals.

Informed consent None.

References

- Ajayi AE, Holthusen D, Horn R (2016) Changes in microstructural behaviour and hydraulic functions of biochar amended soils. *Soil Tillage Res* 155:166–175
- ASTM D422–63 (1998) Standard test method for particle-size analysis of soils. ASTM International, West Conshohocken PA
- ASTM D1762–84 (2007) Standard test method for chemical analysis of wood charcoal. ASTM International, West Conshohocken PA
- Bareither CA, Benson CH, Rohlf E M, IV JS (2020) Hydraulic and mechanical behavior of municipal solid waste and high-moisture waste mixtures. *Waste Manag* 105:540–549
- Barnes RT, Gallagher ME, Masiello CA, Liu ZL (2014) Biochar-induced changes in soil hydraulic conductivity and dissolved nutrient fluxes constrained by laboratory experiments. *PLoS ONE* 9(9):e108340 1–9
- Chen M, Dai J, Liu X, Kang Y, Qin MJ, Wang ZT (2019) Contributions of pore-throat size distribution to reservoir quality and fluid distribution from NMR and MIP in tight sandy conglomerate reservoirs. *Arab J Geosci* 12(1):1–12
- Coates GR, Xiao LL, Prammer MG (1999) NMR logging principles and application. Halliburton Energy Services Publication, Houston
- Chen B, Sun DA, Gao Y, Li J (2017) Experimental study of pore-size distribution of Shanghai soft clay. *Rock Soil Mech* 38(9):2523–2530
- Devereux RC, Sturrock CJ, Mooney SJ (2012) The effects of biochar on soil physical properties and winter wheat growth. *Earth and Environmental Science Transactions of the Royal Society of Edinburgh* 103(1):13–18
- Dunn KJ, Bergman DJ, Latorraca GA (2002) Nuclear magnetic resonance petrophysical and logging applications. Pergamon
- Fang T, Zhang LK, Liu NG, Zhang LQ, Wang WM, Yu L, Li C, Lei YH (2018) Quantitative characterization of pore structure of the Carboniferous–Permian tight sandstone gas reservoirs in eastern Linqing depression by using NMR technique. *Petroleum Research* 3(2):110–123
- Fei YH, She DL, Gao L (2019) Micro-CT assessment on the soil structure and hydraulic characteristics of saline/sodic soils subjected to short-term amendment. *Soil Tillage Res* 193(10):59–70
- GB 51220–2017 (2017) Technical code for municipal solid waste sanitary landfill closure. China Building Industry Press, Beijing
- Garg A, Ng CWW (2015) Investigation of soil density effect on suction induced due to root water uptake by *Schefflera heptaphylla*. *J Plant Nutr Soil Sci* 178(4):586–591
- Horn R, Peng XH, Fleige H, Jose D (2014) Pore rigidity in structured soils—only a theoretical boundary condition for hydraulic properties? *Soil Science and Plant Nutrition* 60(1):3–14

- He YB, Gu F, Xu C, Wang Y (2019) Assessing of the influence of organic and inorganic amendments on the physical-chemical properties of a red soil (Ultisol) quality. *Catena* 183:1–10
- Jeffery S, Verheijen FGA, Veldt MVD, Bostos AC (2011) A quantitative review of the effects of biochar application to soils on crop productivity using meta-analysis. *Agric Ecosyst Environ* 144(1):175–187
- Jaeger F, Bowe S, Vanas H, Schaumann GE (2009) Evaluation of ^1H NMR relaxometry for the assessment of pore-size distribution in soil samples. *Eur J Soil Sci* 60(6):1052–1064
- Jirku V, Kodesova R, Nikodem A, Muhlhanselova M, Zigova A (2013) Temporal variability of structure and hydraulic properties of topsoil of three soil types. *Geoderma* 204–205:43–58
- Kwon O, Cho W (2011) Field applicability of self-recovering sustainable liner as landfill final cover. *Environ Earth Sci* 62(8):1567–1576
- Kong LM, Wang YS, Sun WJ, Qi JL (2020) Influence of plasticity on unfrozen water content of frozen soils as determined by nuclear magnetic resonance. *Cold Regions Science & Technology* 102993
- Laird DA, Fleming P, Davis D, Horton R, Wang BQ, Karlen DL (2010) Impact of biochar amendments on the quality of a typical Midwestern agricultural soil. *Geoderma* 158:443–449
- Lu SG, Sun FF, Zong YT (2014) Effect of rice husk biochar and coal fly ash on some physical properties of expansive clayey soil (Vertisol). *Catena* 114:37–44
- Lei OY, Zhang RD (2013) Effects of biochars derived from different feedstocks and pyrolysis temperatures on soil physical and hydraulic properties. *Journal of Soil & Sediments* 13(9):1561–1572
- Oguntunde PG, Abiodun BJ, Ajayi AE, Giesen NVD (2010) Effects of charcoal production on soil physical properties in Ghana. *Journal of Plant Nutrition & Soil Science* 171(4):591–596
- Peng XY, Tong XG, Hao LT, Wu FQ (2019) Applicability of biochar for limiting interrill erosion and organic carbon export of sloping cropland in a semi-arid area of China. *Agric Ecosyst Environ* 280:68–76
- Prammer MG, Drack ED, Bouton JC, Gardner JS (1996) Measurements of clay-bound water and total porosity by magnetic resonance logging. *SPE* 36522:311–320
- Tian HH, Wei CF, Wei HZ, Yan RT, Chen P (2013) An NMR-based analysis of soil-water characteristics. *Appl Magn Reson* 45(1):49–61
- US EPA (1989) Technical guidance document: final covers on hazardous waste landfills and surface impoundments. US Environmental Protection Agency Washington
- Villagra-Mendoza K, Horn R (2018) Effect of biochar addition on hydraulic functions of two textural soils. *Geoderma* 326:88–95
- Wong JTF, Chen Z, Wong AYY, Ng CWW, Wong MH (2018) Effects of biochar on hydraulic conductivity of compacted kaolin clay. *Environ Pollut* 234:468–472
- Xi K, Cao Y, Haile BG, Zhu RK, Jähren J, Bjørlykke K, Zhang XX, Helleveing H (2016) How does the pore-throat size control the reservoir quality and oiliness of tight sandstones? The case of the lower cretaceous quantou formation in the southern Songliao Basin, China. *Mar Pet Geol* 76:1–15
- Yaghoubi P (2011) Development of biochar-amended landfill cover for landfill gas mitigation. University of Illinois at Chicago
- Yu HH, Sun DA, Tian HH (2019) NMR-based analysis of shear strength of weakly expansive clay in sodium chloride solution. *Magn Reson Imaging* 58:6–13
- Zornoza R, Moreno-Barriga E, Acosta JA, Munoz MA (2016) Stability, nutrient availability and hydrophobicity of biochars derived from manure, crop residues, and municipal solid waste for their use as soil amendments. *Chemosphere* 144:122–130
- Zhao D, Huang S, Huang JS (2015a) Effects of biochar on hydraulic parameters and shrinkage-swelling rate of silty clay. *Transactions of the Chinese Society of Agricultural Engineering* 31(17):136–143
- Zhao HW, Ning ZF, Wang Q, Zhang R, Zhao TY, Niu TF, Zeng Y (2015b) Petrophysical characterization of tight oil reservoirs using pressure-controlled porosimetry combined with rate-controlled porosimetry. *Fuel* 154:233–242
- Zhang S, Zhou XL, Zheng KR, Xie YJ, Fu Q (2014) Characterization of pore structure of hardened cement-asphalt paste by mercury intrusion porosimetry. *Adv Mater Res* 1004–1005:1589–1593

Publisher's note Springer Nature remains neutral with regard to jurisdictional claims in published maps and institutional affiliations.